

# Protein kinase inhibitor ceritinib blocks ectonucleotidase CD39 – a promising target for cancer immunotherapy

Laura Schäkel <sup>1</sup>, Salahuddin Mirza <sup>1</sup>, Riekje Winzer <sup>2</sup>, Vittoria Lopez <sup>1</sup>,  
Riham Idris <sup>1</sup>, Haneen Al-Hroub <sup>1</sup>, Julie Pelletier,<sup>3</sup> Jean Sévigny <sup>3,4</sup>,  
Eva Tolosa,<sup>2</sup> Christa E Müller <sup>1</sup>

**To cite:** Schäkel L, Mirza S, Winzer R, *et al.* Protein kinase inhibitor ceritinib blocks ectonucleotidase CD39 – a promising target for cancer immunotherapy. *Journal for ImmunoTherapy of Cancer* 2022;10:e004660. doi:10.1136/jitc-2022-004660

Accepted 24 May 2022

## ABSTRACT

**Background** An important mechanism, by which cancer cells achieve immune escape, is the release of extracellular adenosine into their microenvironment. Adenosine activates adenosine A<sub>2A</sub> and A<sub>2B</sub> receptors on immune cells constituting one of the strongest immunosuppressive mediators. In addition, extracellular adenosine promotes angiogenesis, tumor cell proliferation, and metastasis. Cancer cells upregulate ectonucleotidases, most importantly CD39 and CD73, which catalyze the hydrolysis of extracellular ATP to AMP (CD39) and further to adenosine (CD73). Inhibition of CD39 is thus expected to be an effective strategy for the (immuno)therapy of cancer. However, suitable small molecule inhibitors for CD39 are not available. Our aim was to identify drug-like CD39 inhibitors and evaluate them in vitro.

**Methods** We pursued a repurposing approach by screening a self-compiled collection of approved, mostly ATP-competitive protein kinase inhibitors, on human CD39. The best hit compound was further characterized and evaluated in various orthogonal assays and enzyme preparations, and on human immune and cancer cells.

**Results** The tyrosine kinase inhibitor ceritinib, a potent anticancer drug used for the treatment of anaplastic lymphoma kinase (ALK)-positive metastatic non-small cell lung cancer, was found to strongly inhibit CD39 showing selectivity versus other ectonucleotidases. The drug displays a non-competitive, allosteric mechanism of CD39 inhibition exhibiting potency in the low micromolar range, which is independent of substrate (ATP) concentration. We could show that ceritinib inhibits ATP dephosphorylation in peripheral blood mononuclear cells in a dose-dependent manner, resulting in a significant increase in ATP concentrations and preventing adenosine formation from ATP. Importantly, ceritinib (1–10 µM) substantially inhibited ATP hydrolysis in triple negative breast cancer and melanoma cells with high native expression of CD39.

**Conclusions** CD39 inhibition might contribute to the effects of the powerful anticancer drug ceritinib. Ceritinib is a novel CD39 inhibitor with high metabolic stability and optimized physicochemical properties; according to our knowledge, it is the first brain-permeant CD39 inhibitor. Our discovery will provide the basis (i) to develop more potent and balanced dual CD39/ALK inhibitors, and (ii) to optimize the ceritinib scaffold towards interaction with CD39 to obtain potent and selective drug-like CD39 inhibitors for future in vivo studies.

## WHAT IS ALREADY KNOWN ON THIS TOPIC

⇒ Ceritinib is an inhibitor of anaplastic lymphoma kinase and an approved anticancer drug.

## WHAT THIS STUDY ADDS

⇒ Herein, we demonstrate that ceritinib additionally acts as a non-competitive inhibitor of the ATP-hydrolyzing ectonucleotidase CD39 showing micromolar potency. It therefore results in decreased extracellular concentrations of immunosuppressive, cancer-promoting adenosine.

## HOW THIS STUDY MIGHT AFFECT RESEARCH, PRACTICE OR POLICY

⇒ In contrast to other investigated kinase inhibitors, ceritinib may have additional immunotherapeutic effects. Moreover, the ceritinib scaffold could be further optimized to obtain more potent CD39 inhibitors for the immunotherapy of cancers.



© Author(s) (or their employer(s)) 2022. Re-use permitted under CC BY-NC. No commercial re-use. See rights and permissions. Published by BMJ.

<sup>1</sup>Pharmaceutical & Medicinal Chemistry, University of Bonn, Bonn, Germany

<sup>2</sup>Immunology, University Medical Center Hamburg-Eppendorf, Hamburg, Germany

<sup>3</sup>Centre de Recherche du CHU de Québec - Université Laval, Québec City, Québec, Canada

<sup>4</sup>Département de Microbiologie-Infectiologie et d'Immunologie, Faculté de Médecine, Université Laval, Québec City, Québec, Canada

## Correspondence to

Professor Christa E Müller;  
christa.mueller@uni-bonn.de

## INTRODUCTION

An important mechanism, by which cancer cells achieve immune escape, is the hypoxia-induced upregulation of ectonucleotidases by hypoxia-inducible factor 1 $\alpha$  (HIF-1 $\alpha$ ) and specific protein 1 (SP-1), resulting in high concentrations of extracellular adenosine in their microenvironment (see [figure 1](#)).<sup>1,2</sup> Adenosine, by activating A<sub>2A</sub> and A<sub>2B</sub> receptors on immune cells, constitutes one of the strongest immunosuppressive mediators.<sup>3–8</sup> The hypoxia–A<sub>2A</sub>–adenosinergic pathway was demonstrated to impede the recruitment and activity of antitumor T cells in the tumor microenvironment.<sup>9</sup> In previous studies, this immunosuppressive hypoxia–A<sub>2A</sub>–adenosinergic signaling was successfully blocked by a specific adenosine A<sub>2A</sub> receptor antagonist, providing the proof of concept that the pharmaceutical reactivation of tumor-reactive T and natural killer cells is feasible.<sup>10,11</sup> In addition, extracellular adenosine promotes cancer cell proliferation, angiogenesis, and metastasis.<sup>5</sup>

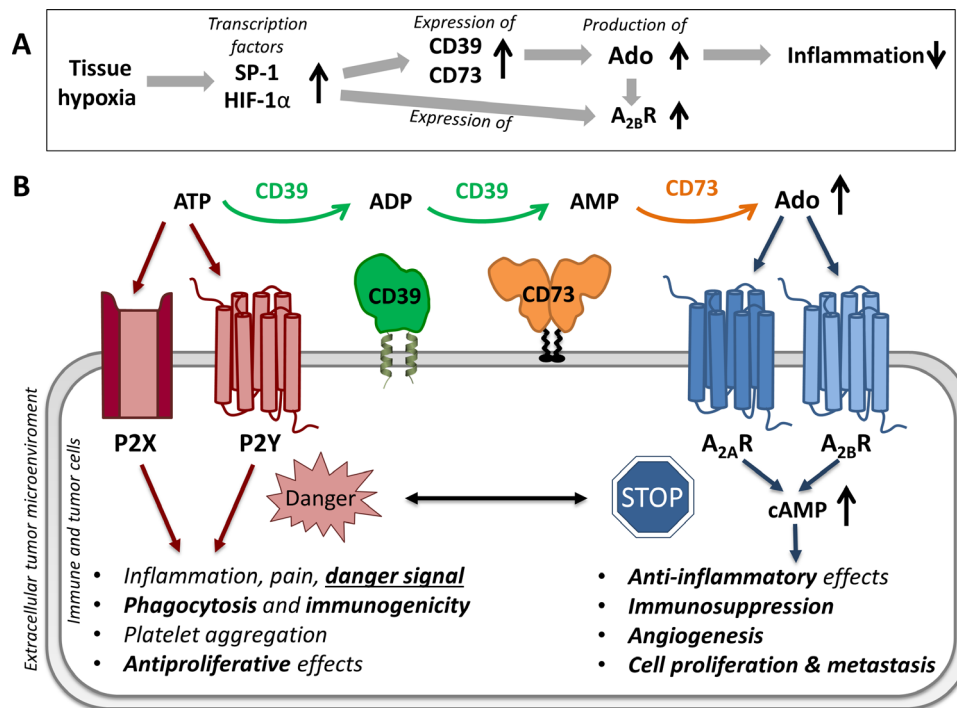


**Figure 1** Hypoxia-induced purinergic signaling. (A) Tissue hypoxia increases the release of transcription factor SP-1 and hypoxia-inducible factor 1 $\alpha$  (HIF-1 $\alpha$ ), which leads to an increase in the expression and enzymatic capacity of adenosine-producing ectonucleotidases and to an increased expression of adenosine A<sub>2B</sub> receptors (A<sub>2B</sub>R), resulting in reduced inflammation.<sup>2</sup> (B) Effects of extracellular adenosine triphosphate (ATP, danger-associated molecular pattern molecule) and adenosine via purinergic P2 and adenosine A<sub>2A</sub> and A<sub>2B</sub> receptors. ATP is dephosphorylated by a concerted action of ectonucleoside triphosphate diphosphohydrolase 1 (NTPDase1, CD39) and ecto-5'-nucleotidase (CD73) to adenosine. SP-1, specific protein 1; CD, cluster of differentiation.

In this context, ectonucleotidases have been proposed as novel targets in immuno-oncology. These membrane proteins catalyze the extracellular dephosphorylation of nucleotides, such as ATP, ADP and AMP, producing adenosine (figure 2). They thereby reduce extracellular concentrations of pro-inflammatory, antiproliferative

ATP, leading to an increase in immunosuppressive, cancer-promoting adenosine.<sup>12–14</sup> This enzymatic cascade constitutes an endogenous feedback loop protecting from ischemia and excessive inflammation, but it can be hijacked by tumors, bacteria, and possibly also by viruses.<sup>2,6,15</sup>

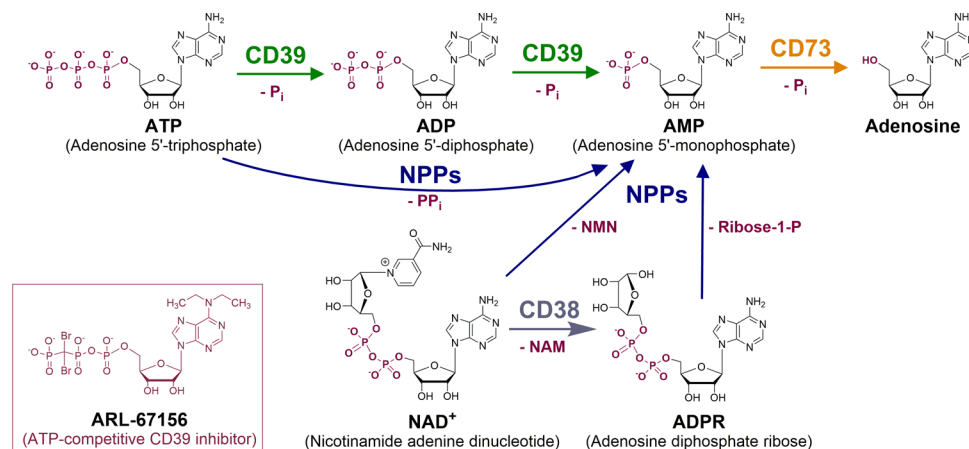


**Figure 2** Generation of adenosine through extracellular hydrolysis of adenine nucleotides by ectonucleotidases. Nucleoside triphosphate diphosphohydrolase-1 (NTPDase1, CD39) and nucleotide pyrophosphatase/phosphodiesterase-1 (CD203a, NPP1, PC-1) as well as their isoenzymes produce AMP, which is hydrolyzed by ecto-5'-nucleotidase (CD73) to yield adenosine. In the course of the reactions, inorganic phosphate (P<sub>i</sub>), or diphosphate (pyrophosphate, PP<sub>i</sub>), is released. As an alternative source for AMP, NAD<sup>+</sup> is converted by the enzyme CD38 to nicotinamide (NAM) and ADP-ribose (ADPR). ADPR can be converted to AMP and ribose-1-phosphate (ribose-1-P) by NPP1 and NPP3. NPPs can also directly transform NAD<sup>+</sup> to AMP by cleaving off nicotinamide mononucleotide (NMN). The ATP analog ARL-67156 is the current standard CD39 inhibitor.<sup>30–32</sup>

The most abundant ATP-hydrolyzing ectonucleotidase is nucleoside triphosphate diphosphohydrolase-1 (NTPDase1, CD39), which converts ATP via ADP to AMP. Further cell membrane-bound ecto-NTPDase isoenzymes include NTPDase2, -3, and -8, while all other NTPDases are located on intracellular organelles.<sup>16</sup> Alternatively, extracellular AMP can be produced by nucleotide pyrophosphatase/phosphodiesterases (NPPs), a promiscuous enzyme family that catalyzes the hydrolysis of various nucleotides. The main NPP isoenzyme, NPP1 (CD203a, PC-1) hydrolyzes ATP, nicotinamide mononucleotide (NAD<sup>+</sup>), ADP-ribose (ADPR) and dinucleoside triphosphates and tetraphosphates.<sup>17–22</sup> In addition, NAD<sup>+</sup> can be hydrolyzed by CD38 yielding ADPR, which may then be degraded to AMP by NPP1. AMP produced by CD39 and NPPs is further hydrolyzed by ecto-5'-nucleotidase (CD73) yielding adenosine.<sup>23</sup> Adenosine signaling is modulated by additional pathways. For example, ubiquitously expressed alkaline phosphatase and prostate-specific phosphatase are also able to generate adenosine from AMP.<sup>1</sup> Adenosine can be deaminated by adenosine deaminases (ADA1 and ADA2) to inosine, or phosphorylated by adenosine kinase regenerating the nucleotide AMP. The extracellular concentration of adenosine is additionally regulated by equilibrative nucleoside transporters (e.g. ENT1 and ENT2) and by concentrative nucleoside transporters.<sup>1,2</sup>

CD39, NPP1 and CD73 are upregulated on many types of cancer, providing an immunosuppressive, cancer proliferation-promoting environment. CD73 has even been proposed as a diagnostic marker in metastatic melanoma.<sup>24,25</sup>

Several anti-hypoxia-adenosinergic drugs are currently in clinical development for the immunotherapy of cancer.<sup>26</sup> Besides adenosine A<sub>2A</sub> receptor antagonists, a small molecule CD73 inhibitor and several antibodies are currently evaluated in clinical trials.<sup>27</sup> Inhibition of CD39 might be even more powerful since the resulting increase in ATP and the expected decrease in AMP, the substrate for adenosine generation by CD73, is expected to be synergistic.<sup>13,28,29</sup>

So far, only moderately potent and/or non-selective and metabolically unstable CD39 inhibitors have been described.<sup>30–38</sup> For example, the currently preferred standard CD39 inhibitor, ARL-67156, which has been and is still used in many *in vitro* and *in vivo* studies,<sup>39–43</sup> displays a K<sub>i</sub> value in the micromolar range at human CD39.<sup>31,32</sup> This nucleotide analog (figure 2) is a competitive inhibitor showing similarity to the substrate ATP. The ATP cleavage site for dephosphorylation by NTPDases between the β- and γ-phosphate groups is stabilized in ARL-67156 by a dibromomethylene bridge. ARL-67156 was recently shown to be non-selective, also inhibiting CD73 even with higher potency (K<sub>i</sub> value of 0.451 μM), and to be metabolically unstable upon incubation with human and mouse liver microsomes; it is therefore not suitable for *in vivo* studies.<sup>32</sup> The optimization of nucleotidic CD39 inhibitors such as ARL-67156 acting as substrate analogs has so far met with limited success.<sup>32</sup>

In the present study, we pursued a completely new approach to identify novel CD39 inhibitors – the screening of approved ATP-competitive protein kinase inhibitory drugs. Protein kinase inhibitors constitute a growing class of therapeutics for targeted cancer therapy.<sup>44–46</sup> Most of the developed and approved inhibitors block the co-substrate binding site for ATP in a competitive manner. Since CD39 harbors a binding site for its substrate ATP, we figured that some of the ATP-competitive protein kinase inhibitors might also inhibit this extracellularly accessible ecto-enzyme. Hit compounds discovered within a library of approved drugs could be an excellent starting point for further optimization due to their already ideal pharmacokinetic and further drug-like properties. Thus, we collected a library of approved therapeutic drugs targeting the ATP binding site of protein kinases, and screened them for CD39 inhibition. This led to the discovery of ceritinib, belonging to a new chemotype of CD39 inhibitors.

## METHODS

### Assembly of an approved protein kinase inhibitor library

Small molecule protein kinase inhibitors were collected that were approved either by the US Food and Drug Administration (FDA) (<http://www.fda.gov/oc/oc/pkls/pkls.htm>, version of 12.04.2019), or by the European Medicines Agency and available in Germany (<https://www.pharmazeutische-zeitung.de/ausgabe-132018/sortierendes-grossen-sortiments/>). At the time of collection, the library contained a total of 50 drug molecules. All compounds were purchased from Sigma Aldrich (Darmstadt, Germany), with the exception of netarsudil, which was not commercially available (see table 1).

### Materials

1,N<sup>6</sup>-etheno-ATP, etheno-ADP, etheno-AMP, and etheno-adenosine (eATP, eADP, eAMP, and eADO) were purchased from BIOLOG Life Science Institute (Bremen, Germany). Disodium hydrogenphosphate, lanthanum chloride, sodium acetate, sodium chloride and sulfuric acid were obtained from Carl Roth (Karlsruhe, Germany). [2,8-<sup>3</sup>H]AMP (solution in ethanol/water, 1:1, 22.9 Ci/mmol, 1.0 mCi/ml, 849 GBq/mmol) was purchased from Hartmann Analytic (Braunschweig, Germany). ATP, ammonium heptamolybdate, Brij L23, calcium chloride, dimethyl sulfoxide (DMSO), dipyrindamole, magnesium chloride, malachite green, 4-(2-hydroxyethyl)piperazine-1-ethanesulfonic acid (HEPES) and polyvinyl alcohol were obtained from Sigma (Steinheim, Germany).

Dulbecco's Modified Eagle's Medium (DMEM), fetal calf serum (FCS), penicillin/streptomycin (P/S), and L-glutamine were purchased from Gibco BRL, Gaithersburg, Maryland, USA. RPMI-1640 culture medium was from PAN Biotech GmbH. Cellfectin II reagent (Thermo Fisher Scientific, Massachusetts, USA), baculovirus genomic ProEasy vector DNA (AB vector, California, USA), Insect-XPRESS media (#: BE12-730Q,

**Table 1** Collection of protein kinase inhibitors used for CD39 screening

#	Drug	Trade name	CAS-number	Target
1	Abemaciclib	Verzenio	1231929-97-7	CDK4/6
2	Acalabrutinib	Calquence	1420477-60-6	Bruton tyrosine kinase
3	Afatinib	Tovok	850140-72-6	EGFR, ErbB2, ErbB4
4	Alectinib	Alecensa	1256580-46-7	ALK and RET
5	Axitinib	Inlyta	319460-85-0	VEGFR1/2/3, PDGFR $\beta$
6	Baricitinib	Olumiant	1187594-09-7	JAK1/2
7	Binimetinib	Mektovi	606143-89-9	MEK1/2
8	Bosutinib	BOSULIF	380843-75-4	BCR-Abl, Src, Lyn, and Hck
9	Brigatinib	Alunbrig	1197953-54-0	ALK, ROS1, IGF-1R, Flt3, EGFR
10	Cabozantinib	Cometriq	849217-68-1	RET, MET, VEGFR1/2/3, Kit, TrkB, Flt3, Axl, Tie2
11	Ceritinib	Zykadia	1032900-25-6	ALK, IGF-1R, InsR, ROS1
12	Cobimetinib	Cotellic	934660-93-2	MEK1/2
13	Crizotinib	Xalkori	877399-52-5	ALK, MET (HGFR), ROS1, MST1R
14	Dabrafenib	Tafinlar	1195765-45-7	B-Raf
15	Dacomitinib	Visimpro	1110813-31-4	EGFR family
16	Dasatinib	Sprycel	302962-49-8	BCR-Abl, EGFR, Src, Lck, Yes, Fyn, Kit, EphA2, PDGFR $\beta$
17	Encorafenib	Braftovi	1269440-17-6	B-Raf
18	Erdafitinib	Balversa	1346242-81-6	FGFR1/2/3/4
19	Erlotinib	Tarceva	183319-69-9	EGFR
20	Everolimus	Afinitor	159351-69-6	FKBP12/mTOR
21	Fostamatinib	Tavalisse	901119-35-5	Syk, Spleen tyrosine kinase
22	Gefitinib	Iressa	184475-35-2	EGFR
23	Gilteritinib	Xospata	1254053-43-4	Flt3
24	Ibrutinib	Imbruvica	936563-96-1	Bruton tyrosine kinase
25	Idelalisib	Zydelig	870281-82-6	Phosphatidylinositol-3- Kinase
26	Imatinib	Gleevec	152459-95-5	BCR-Abl, Kit, and PDGFR
27	Lapatinib	Tykerb	231277-92-2	EGFR, ErbB2
28	Larotrectinib	Vittrakvi	1223403-58-4	TRK
29	Lenvatinib	Lenvima	417716-92-8	VEGFR1/2/3, PDGFR, FGFR, Kit, RET
30	Lorlatinib	Lorbrena	1454846-35-5	ALK
31	Midostaurin	Rydapt	120685-11-2	Flt3, PDGFR, VEGFR2, PKC
32	Neratinib	Nerlynx	698387-09-6	ErbB2/HER2
33	Nilotinib	Tasigna	641571-10-0	BCR-Abl, PDGFR, DDR1
34	Nintedanib	Vargatef	656247-17-5	FGFR1/2/3, PDGFR $\alpha/\beta$ , VEGFR1/2/3, Flt3
35	Osimertinib	Tagrisso	1421373-65-0	EGFR T970M
36	Palbociclib	Ibrance	571190-30-2	CDK4/6
37	Pazopanib	Votrient	444731-52-6	VEGFR1/2/3, PDGFR $\alpha/\beta$ , FGFR1/3, Kit, Lck, Fms, Itk
38	Ponatinib	Iclusig	943319-70-8	BCR-Abl, BCR-Abl T315I, VEGFR, PDGFR, FGFR, EphR, Src family kinases, Kit, RET, Tie2, Flt3
39	Regorafenib	Stivarga	755037-03-7	VEGFR1/2/3, BCR-Abl, B-Raf, B-Raf (V600E), Kit, PDGFR $\alpha/\beta$ , RET, FGFR1/2, Tie2, and Eph2A

Continued

**Table 1** Continued

#	Drug	Trade name	CAS-number	Target
40	Ribociclib	Kisqali	1211441-98-3	CDK4/6
41	Ruxolitinib	Jakafi	941678-49-5	JAK1/2
42	Sirolimus	Rapamycin	53123-88-9	FKBP/mTOR
43	Sorafenib	Nexavar	284461-73-0	VEGFR1/2/3, B-/C-Raf, mutant B-Raf, Kit, FIt3, RET, and PDGFR $\beta$
44	Sunitinib	Sutent	557795-19-4	PDGFR $\alpha/\beta$ , VEGFR1/2/3, Kit, FIt3, CSF-1R, Axl, and RET
45	Temsirolimus	Torisel	162635-04-3	FKBP12/mTOR
46	Tivozanib	Fotivda	475108-18-0	Multikinase inhibitor, eg, VEGF receptor tyrosine kinase
47	Tofacitinib	Tasocitinib	477600-75-2	JAK3
48	Trametinib	Mekinist	871700-17-3	MEK1/2
49	Vandetanib	Zactima	443913-73-3	RET, EGFRs, VEGFRs, Brk, Tie2, EphRs, and Src family kinases
50	Vemurafenib	Zelboraf	918504-65-1	A/B/C-Raf and B-Raf (V600E)

Lonza, Switzerland) and HisPur Ni<sup>2+</sup>-NTA spin columns (#: 88226, Thermo Fisher Scientific, Massachusetts, USA) were used as protein expression and purification tools. For capillary electrophoresis, polyacrylamide-coated capillaries were purchased from Chromatographie Service GmbH (Langerwehe, Germany).

## Enzyme preparations

### Recombinant expression of enzymes

Human NTPDase-1, -2, -3 and -8 were recombinantly expressed in COS-7 cells (a non-human primate cell line, CV-1 in Origin with SV40 genes), and membrane preparations were obtained according to published protocols.<sup>33 47–49</sup> The human cDNAs for the enzymes NPP1, NPP3, NPP4, NPP5, CD38 and CD73 (Genbank accession no. cDNA sequences NM\_006208, NM\_005021, NM\_021572, NM\_014936, NM\_001775, and NM\_002526, respectively) were obtained from Origene (Rockville, USA). Soluble enzymes were produced as previously reported.<sup>32 36 50</sup> The plasmids contained the catalytic domains of the enzymes to which a 9× histidine tag (His-tag) was added at the C-terminus (except for NPP1, which was expressed without tag), in addition to the expression vector pACGP67 A/B. Sf9 insect cells were transfected using Cellfectin II Reagent (Thermo Fisher Scientific, Massachusetts, USA) and ProEasy baculovirus linearized DNA (Cat.#A10S, AB Vector). The expressed protein was released into the supernatant and collected after 48 hours of incubation at 27°C. The enzymes were purified using HisPur Ni<sup>2+</sup>-NTA spin columns according to the manufacturer's protocol. The protein concentration was determined by the Lowry method.<sup>51</sup>

### Preparation of umbilical cord membranes natively expressing CD39

Human umbilical cord membrane preparations were obtained as previously reported.<sup>52</sup> In brief, tissue samples

were homogenized with a polytron, filtered through a cheesecloth, and centrifuged to remove debris and nuclei. Membrane protein fractions were collected from the pellets obtained after ultracentrifugation. All purification steps were performed at 4°C. Protein stock solutions were aliquoted and stored at -80°C until use in the assays.

### Isolation of human peripheral blood mononuclear cells

Buffy coats were obtained from the blood bank of the University Medical Center Hamburg-Eppendorf. Peripheral blood mononuclear cells (PBMCs) were isolated by Biocoll (Merck) density gradient centrifugation. Blood was diluted with phosphate-buffered saline (PBS) (Thermo Fisher Scientific) and carefully layered on Biocoll. After centrifugation (25 min, 800 g, RT, the lymphocyte layer was collected and washed twice with cold PBS (650 g, 10 min, 4°C, and 450 g, 5 min, 4°C). The expression of CD39 and CD73 on PBMCs was assessed by flow cytometry.

### Membrane preparations of human cancer cells

Membrane preparations of human triple-negative breast cancer (TNBC, MDA-MB-231) and melanoma (Ma-Mel-65) cells were prepared as follows. Once cells had reached a confluency of ca. 90%, cells of one 175 cm<sup>2</sup> flask were passed into 20 sterile 150 mm dishes and incubated at 37°C, 5% CO<sub>2</sub>. After the cells had grown into a monolayer of ~90% confluency, the medium was decanted, dishes were rinsed with 5 mL of PBS and frozen at -20°C. Frozen cells were scraped off the dishes with 1 mL of an ice-cold buffer consisting of 25 mM Tris-HCl, 1 mM EDTA, 0.32 M saccharose and 100 μM phenylmethylsulfonyl fluoride (protease inhibitor) at pH 7.4 with a cell scraper. This step was repeated to ensure that all cells were collected from each dish. All cells were transferred to a beaker, and the cell suspension was treated with an Ultraturrax (twice, 30 s each at high speed). To remove nuclei, other

larger organelles, and cell debris, the homogenate was centrifuged at 1000 g for 10 min (4°C). The supernatant was collected and subsequently centrifuged at 48,000 g for 1 hour (4°C). The obtained pellets were resuspended in washing buffer and centrifuged using the same conditions. After two more washing steps, the pellets were resuspended in 0.1 mL per dish of 50 mM Tris-HCl buffer, pH 7.4, and the crude membrane suspensions were stored at -80°C until use. All steps were carried out as fast as possible at a temperature of 4°C to avoid enzyme internalization. Protein concentrations were determined using the Lowry assay.<sup>51</sup> The determined protein concentration was 10.0 µg/µL for TNBC and 9.1 µg/µL for melanoma cell membrane preparations.

### Cell culture and monitoring of nucleotide hydrolysis on cancer cells

Human TNBC cells (MDA-MB-231) were grown in DMEM medium supplemented with 10% FCS, and 1% P/S at 37°C and 10% CO<sub>2</sub>. Melanoma (MaMel65) cell lines were cultured in RPMI-1640 medium with 10% FCS, 1% P/S, and 1% L-glutamine at 37°C and 5% CO<sub>2</sub>. Cells were harvested using trypsin, washed three times using reaction buffer consisting of 10 mM HEPES, pH 7.4, 2 mM CaCl<sub>2</sub>, and 1 mM MgCl<sub>2</sub>. The hydrolysis of eATP to its product eADO by the concerted action of CD39 and CD73 overexpressed on these cells was monitored. eADO was quantified after precipitation of the nucleotides (eATP, eADP, and eAMP) using LaCl<sub>3</sub> (a detailed assay procedure will be published elsewhere). Briefly, 300,000 cells/reaction (pretreated for 30 min with 20 µM of the nucleoside transport inhibitor dipyrindamole)<sup>53</sup> were incubated with or without ceritinib (100, 10, or 1 µM) for 1 hour at 37°C. The reaction was terminated by the addition of precipitation buffer consisting of 14.2 mM NaH<sub>2</sub>PO<sub>4</sub> and 71.7 mM LaCl<sub>3</sub>/NaOAc under acidic conditions. Then, the samples were centrifuged at 1200 rpm for 10 min. The uncharged eADO remained in the supernatant while the nucleotides were precipitated. Aliquots of 100 µL of supernatant were then transferred to a fresh half area 96-well plate. Relative fluorescence units (at 300/410 nm) were measured by a fluorescence microplate reader (Flexstation, Medical Devices, USA).

### Malachite green assay for measuring NTPDase activity (CD39 and NTPDases2, -3 and 8)

Effects of compounds on ATP hydrolysis by CD39, NTPDase2, -3 or -8, and by human cancer cell membrane preparations were evaluated using the malachite green assay.<sup>54</sup> The substrate concentration of ATP was 50 µM for CD39 and the cancer cell membrane preparations, and 100 µM for NTPDase2, -3 or -8. The assay was performed in clear half area plates in a total volume of 50 µL of 10 mM HEPES containing 2 mM CaCl<sub>2</sub> and 1 mM MgCl<sub>2</sub> (pH 7.4) in the presence of a maximal concentration of 2% DMSO. The mixtures of inhibitor and enzyme were preincubated at 37°C

for 5 min. Subsequently, the enzymatic dephosphorylation of ATP was started by addition of the substrate. The samples were incubated at 37°C for 15 min, then the reaction was stopped by adding the malachite green detection reagents (20 µL of malachite green solution (0.6 mM) and 30 µL of ammonium molybdate solution (20 mM) in sulfuric acid (1.5 M)). Absorption of the samples at 600 nm was measured using the BMG PHERAstar FS plate reader (BMG Labtech GmbH, Ortenberg, Germany) after 20 min of incubation at 25°C. The corrected absorption was calculated by subtracting the absorption of the negative control samples, which were incubated with denatured enzyme (90°C, 15 min).

The kinase inhibitors were initially investigated at 10 µM concentration at human CD39, natively expressed in high density in human umbilical cord membrane preparations at a protein concentration of 50.0 ng per well. Further studies were performed using CD39 and the respective NTPDase proteins expressed in COS-7 cell membranes (ca. 100 ng of protein depending on enzymatic activity, adjusted to ensure 10%–20% of substrate conversion).<sup>33, 47</sup> The respective enzyme was incubated with or without 50 µM ceritinib and 50 or 100 µM ATP ( $K_m$  (CD39)=17 µM;  $K_m$  (NTPDase2)=70 µM;  $K_m$  (NTPDase3)=75 µM;  $K_m$  (NTPDase8)=46 µM).<sup>48</sup> Full concentration-inhibition curves were determined with inhibitor concentrations ranging from 0.1 to 300 µM. For the inhibition type experiments, 57.0 ng of recombinant human CD39 was incubated with 0, 5, 10, 15 and 20 µM of ceritinib and increasing substrate (ATP) concentrations of 10, 25, 50, 100 or 150 µM. All experiments were performed in three independent iterations (n=3), and the obtained data were processed and plotted with GraphPad Prism V.8 software (San Diego, USA).

### Capillary electrophoresis assay for monitoring CD39 activity

The effects of ceritinib on CD39 activity were additionally determined by a previously established capillary electrophoresis (CE)-based assay.<sup>52</sup> Briefly, ceritinib in a concentration range of 0.1 to 300 µM was incubated with 100 µM of ATP as substrate ( $K_m$  (CD39)=17 µM) and recombinant human CD39 preparations suspended in reaction buffer consisting of 10 mM HEPES, 2 mM CaCl<sub>2</sub> and 1 mM MgCl<sub>2</sub> (pH 7.4) in a final volume of 100 µL. Incubation at 37°C was performed for 30 min, followed by heating at 90°C for 10 min in order to prevent further enzymatic degradation of the substrate. The nucleotides were separated using a P/ACE MDQ CE system (Beckman Instruments, Fullerton, California, USA) and evaluated with the P/ACE MDQ software V.32 KARAT obtained from Beckman Coulter (Fullerton, California, USA).

### CD73 assay

The effect of ceritinib on soluble human CD73 was determined with a previously established assay.<sup>55</sup> For concentration-inhibition curves of ceritinib, a dilution

series of the compound was incubated at 37°C for 25 min with 0.09 µg/mL of soluble human CD73<sup>50</sup> and 5.0 µM of the radioactive substrate [2,8-<sup>3</sup>H]AMP (specific activity 7.4×10<sup>8</sup> Bq/mmol, 20 mCi/mmol) in a shaking water bath. The assay buffer consisted of 25 mM Tris, 140 mM NaCl and 25 mM NaH<sub>2</sub>PO<sub>4</sub> at pH 7.4. After incubation, 500 µL of cold precipitation buffer (100 mM LaCl<sub>3</sub>, 100 mM sodium acetate, pH 4.0) was added to precipitate free phosphate and unconverted [2,8-<sup>3</sup>H]AMP for 30 min on ice. The filtrate was collected by filtering the samples through GF/B glass fiber filters using a Brandel cell harvester (M-48, Brandel, Maryland, USA). The reaction vials were washed three times each with 400 µL of cold (4°C) demineralized water. Then, 5 mL of scintillation cocktail (ULTIMA Gold XR9) were mixed with aliquots of the filtrate in order to quantify the isolated product of the enzymatic reaction, radioactive adenosine, by liquid scintillation counting (TRICARB 2900 TR, Packard/PerkinElmer).

#### NPP1 assay

The NPP1 enzymatic activity on the degradation of its substrate ATP was evaluated by analyzing the reaction product AMP by CE. A mixture of 800 ng of NPP1 (crude soluble form expressed in Sf9-insect cells),<sup>36</sup> 50 µM of ceritinib, 2% DMSO and 300 µM of ATP as a substrate in reaction buffer (10 mM *N*-cyclohexyl-2-aminoethanesulfonic acid (CHES), pH 9.0, 2 mM CaCl<sub>2</sub>, 1 mM MgCl<sub>2</sub>) were incubated for 30 min at 37°C with gentle shaking. The reaction was terminated by heating at 90°C for 5 min, and afterwards cooled down on ice. The quantitative analysis of the reaction product AMP was performed by CE (AB Sciex, Framingham, USA), according to a published procedure.<sup>56</sup>

#### NPP3 assay

Inhibition of NPP3 was determined as previously described.<sup>57</sup> Purified soluble NPP3 (95 ng per reaction), expressed in Sf9-insect cells,<sup>36</sup> was incubated with ceritinib at a final concentration of 50 µM, 2% DMSO, and 400 µM of the artificial substrate *p*-nitrophenyl thymidine 5'-monophosphate (*p*-Nph-5'-TMP) in a final volume of 100 µL of reaction buffer (50 mM Tris HCl, pH 9.2, 2 mM CaCl<sub>2</sub>, 0.1 mM ZnCl<sub>2</sub>) for 30 min at 37°C with gentle shaking. The enzyme reaction was terminated by the addition of 20 µL of 1 M aq NaOH solution. The absorption of the formed *p*-nitrophenolate anion was measured at 400 nm using a BMG PHERAstar FS plate reader (BMG Labtech GmbH, Ortenberg, Germany).

#### NPP4 assay

The effect on NPP4 activity was tested by employing diadenosine tetraphosphate (AP<sub>4</sub>A) as a substrate, which is cleaved to ATP and AMP by the enzyme. A mixture of 1200 ng of NPP4 (soluble form expressed in Sf9-insect cells and purified),<sup>49</sup> 50 µM of ceritinib, 2% DMSO and 300 µM of AP<sub>4</sub>A as substrate were incubated for 90 min at 37°C in reaction buffer (10 mM HEPES,

2 mM CaCl<sub>2</sub> and 1 mM MgCl<sub>2</sub> (pH 8.0)) with gentle shaking. The reaction was terminated by heating at 90°C for 5 min, and then cooled down on ice. The quantitative analysis of the reaction product ATP was performed by CE (AB Sciex, Framingham, USA), according to a published procedure.<sup>58</sup>

#### NPP5 and CD38 assay

Inhibition of the enzymes by ceritinib was measured using the natural substrate NAD<sup>+</sup>. CD38 (5 ng) or NPP5 (250 ng) were mixed with 50 µM ceritinib and 100 µM NAD<sup>+</sup> in reaction buffer (CD38: 10 mM HEPES, pH 7.4; NPP5: 10 mM CHES (pH 9.0), 2 mM CaCl<sub>2</sub>, 1 mM MgCl<sub>2</sub>) for 30 min at 37°C. The samples were heated to terminate the reaction (10 min at 95°C), and cooled on ice for 10 min. The reaction products, either ADPR (CD38) or AMP (NPP5), were quantified by CE (AB Sciex, Framingham, USA).<sup>58</sup>

#### High performance liquid chromatography for measuring AMPase and ATPase activities on PMBCs

To determine the effect of ceritinib on the ATPase and AMPase activity of human PMBCs, 2×10<sup>5</sup> PMBCs were treated with ceritinib for 15 min at 37°C, and then incubated with 1 µM eATP or eAMP for 30 min at 37°C. After the incubation, cells were removed (450 g, 5 min, 4°C) and all samples were passed through 10 kDa size exclusion filters (10,000 g, 10 min, 4°C, Pall Corporation) and stored at -20°C until analysis. The analysis was performed on a reversed-phase high performance liquid chromatography (HPLC) system (Agilent Technologies) with a 250 mm × 4.6 mm C8 Luna column (5 µm particle size, Phenomenex) as stationary phase. The mobile phase consisted of different compositions of HPLC buffer A (20 mM KH<sub>2</sub>PO<sub>4</sub>, pH 6.0) and B (50% buffer A, 50% methanol), and elution of the nucleotides from the column resulted from an increasing methanol content in the mobile phase (0.0 min (0.0% buffer B), 5.0 min (0.0% buffer B), 27.5 min (100.0% buffer B), 30.0 min (100.0% buffer B), 32.0 min (0.0% buffer B), 43.0 min (0.0% buffer B)). The signals were detected by fluorescence detection (230 nm excitation wavelength, 410 nm emission wavelength). Defined amounts of ethenonucleotides were measured as standards for quantification of eATP, eADP, eAMP and eADO.

#### Statistical analysis of data

All statistical evaluations were performed using GraphPad Prism V.8 software (San Diego, USA). One-way or two-way analysis of variance tests were employed to detect the significant differences between groups, and Dunnett's multiple comparison test was used to compare the respective inhibitor samples to the controls without inhibitor addition. Data were expressed as mean±SEM. P values were represented as asterisks; p values of <0.05 were considered statistically significant: 0.01–0.05, significant (\*); 0.01–0.001, very significant

(\*\*); 0.001–0.0001, highly significant (\*\*\*) ;  $p < 0.0001$ , extremely significant (\*\*\*\*).

## RESULTS

A compound library of protein kinase inhibitors, approved by the US FDA or the European Medicines Agency, was assembled (see [table 1](#)). The compounds were initially tested at a concentration of  $10 \mu\text{M}$  for inhibition of human CD39 natively expressed in umbilical cord membranes ([figure 3](#)). A single hit compound showed an enzyme inhibition of  $>50\%$  (corresponding to a hit rate of 2%), namely ceritinib ([figure 3](#)). Ceritinib is a potent inhibitor of the anaplastic lymphoma kinase (ALK), a receptor tyrosine kinase. The second most potent CD39 inhibitor was the tyrosine kinase inhibitory drug ponatinib ([figure 3](#)) showing a significant inhibition of 33% at  $10 \mu\text{M}$  concentration.

Ceritinib is an FDA-approved drug for the treatment of ALK-positive non-small cell lung cancer. Its  $IC_{50}$  value against ALK was reported to be in the subnanomolar range, and the inhibitor was proposed to be ATP-competitive based on a crystal structure of a related compound.<sup>59 60</sup> Ceritinib is administered perorally up to a maximum daily dose of 750 mg and shows some brain permeation.<sup>61 62</sup> Maximum plasma levels of the drug were reported to be around  $800 \pm 205 \text{ ng per milliliter}$  corresponding to  $1.4 \pm 0.4 \mu\text{M}$ , and the anticancer drug was found to be metabolically highly stable.<sup>61</sup> In a recent study on patients with brain tumors, ceritinib was found to accumulate in tumor tissue, where an average concentration of  $36 \mu\text{M}$  ( $2\text{--}139 \mu\text{M}$ ) was measured after application of the 10<sup>th</sup> applied dose, while the unbound fraction was low.<sup>63</sup>

### Characterization of ceritinib as a CD39 inhibitor

As a next step, we investigated the inhibitory effect of different concentrations of ceritinib on recombinant and umbilical cord membrane-derived CD39 applying two different, orthogonal assays. The malachite green assay allows the quantification of inorganic phosphate released by the CD39-catalyzed hydrolysis of ATP via ADP to AMP. A CE-based assay coupled to ultraviolet (UV) detection (CE-UV) enables the separation and quantification of the nucleotide ATP along with its intermediate and final products ADP and AMP formed by the enzymatic reaction. According to the sensitivities of the different assays, the substrate ATP was employed at a concentration  $50 \mu\text{M}$  in the malachite green assay, while  $100 \mu\text{M}$  of ATP were required for the CE-UV assay. Different human CD39 enzyme preparations were employed, natively expressed CD39 in umbilical cord membrane preparations, and recombinant CD39 expressed in COS-7 cells, respectively. In the malachite green assay on native CD39, an  $IC_{50}$  value of  $11.3 \mu\text{M}$  was determined for ceritinib. A very similar  $IC_{50}$  value of  $13.7 \mu\text{M}$  was obtained in the CE-UV assay at the recombinant enzyme ([figure 4A](#)). The almost identical  $IC_{50}$  values despite a twofold difference in substrate

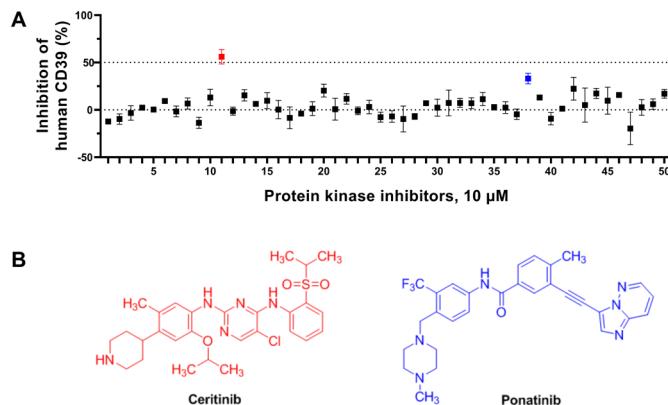


**Figure 3** (A) Screening of a library of approved protein kinase inhibitors for inhibition of human CD39 (expressed in umbilical cord membranes) using the malachite green assay. A concentration of  $10 \mu\text{M}$  of the test compounds was employed. Data points represent means  $\pm$  SEM of three separate experiments. Hit compounds: ceritinib,  $p$  value  $< 0.0001$ ; ponatinib,  $p$  value  $< 0.0478$ . The data were analyzed by one-way analysis of variance and Dunnett's multiple comparison test towards the normalized control without the inhibitors. (B) Structures of approved protein kinase inhibitors identified in a screening approach to significantly block the ectonucleotidase CD39. Ceritinib, a potent anaplastic lymphoma kinase (ALK) inhibitor approved for ALK-positive metastatic non-small cell lung cancer in patients with inadequate clinical response or intolerance to crizotinib,<sup>75</sup> and ponatinib, a multitarget tyrosine kinase inhibitor used for the treatment of chronic myeloid leukemia and Philadelphia chromosome-positive acute lymphoblastic leukemia.<sup>76</sup>

concentrations ( $50 \mu\text{M}$  and  $100 \mu\text{M}$ ) in both assays may hint at a substrate concentration-independent inhibition mechanism ([figure 4A](#)). Subsequent studies were performed to elucidate ceritinib's inhibition type on CD39. To this end,  $K_m$  and  $V_{max}$  values were determined in the absence and in the presence of increasing concentrations of ceritinib. While the inhibitor had no significant effects on the  $K_m$  value of ATP hydrolysis by CD39, the  $V_{max}$  value showed a progressive decrease with increasing concentrations of the inhibitor ([figure 4B–D](#)). This indicates a non-competitive, allosteric inhibition type. A Hanes-Woolf plot was performed that visualizes the non-competitive CD39 inhibition mechanism. A  $K_i$  value of  $11.0 \mu\text{M}$  was calculated from the plotted data which is in excellent agreement with the data obtained in the initial studies using fixed substrate concentrations, where  $IC_{50}$  values of  $11.3$  and  $13.7 \mu\text{M}$  were determined for the native and recombinant forms of CD39, respectively.

Next, ceritinib was studied for potential inhibition of other NTPDase isoenzymes related to CD39, and on further relevant human ectonucleotidases. While NTPDases 3 and –8 were also inhibited by ceritinib at a concentration of  $50 \mu\text{M}$ , NTPDase 2 was not affected. Very low or no inhibition of the ATP-hydrolyzing ectonucleotidase NPP1 and its isoenzymes NPP3, –4, and –5 was observed. Similarly, only moderate inhibition of AMP-hydrolyzing CD73, and of CD38 by ceritinib was detected indicating that the compound is selective for members of



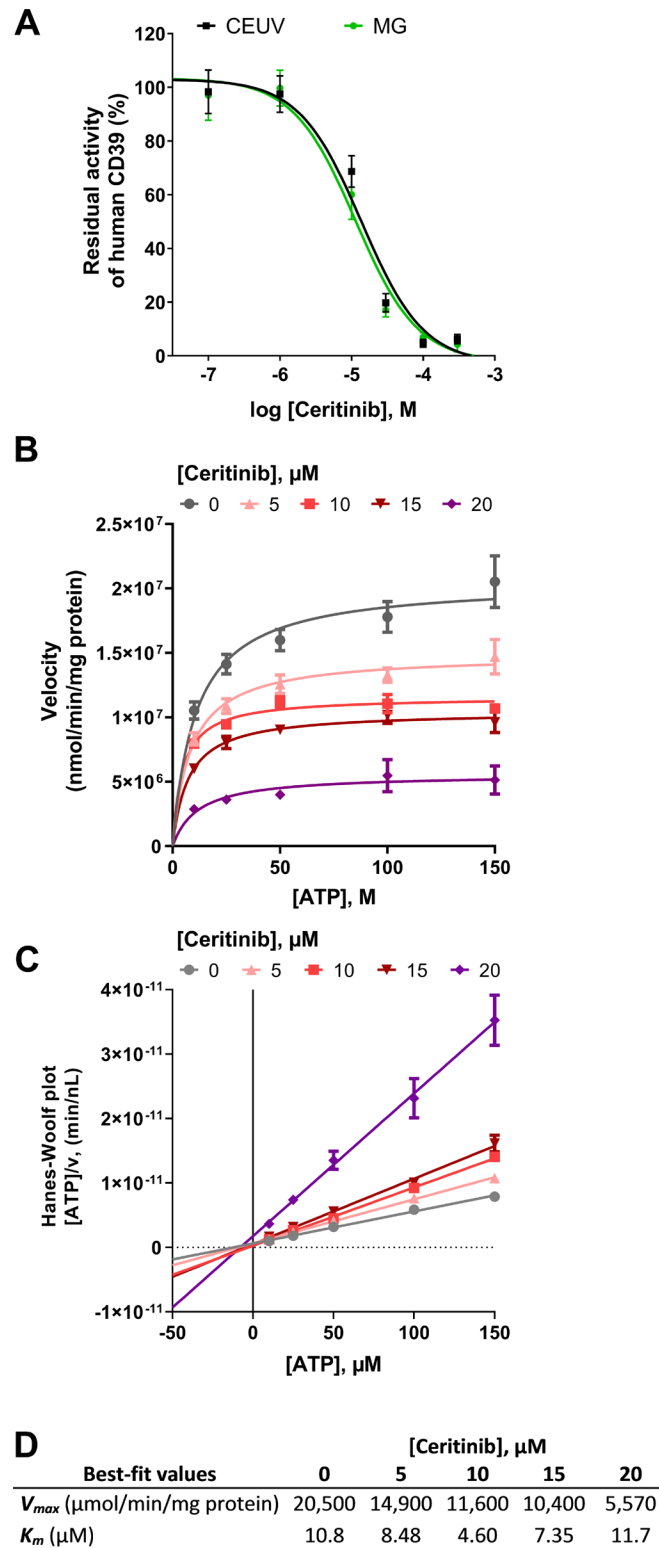


**Figure 4** Characterization of ceritinib as a CD39 inhibitor. (A) Concentration-dependent inhibition of human CD39 by ceritinib determined with the malachite green (MG) assay (green) on human umbilical cord membrane preparations expressing CD39 (ATP substrate concentration of  $50\ \mu\text{M}$ ), and determined with the CE-UV assay (black) on recombinant human CD39 (ATP substrate concentration of  $100\ \mu\text{M}$ ).  $\text{IC}_{50}$ -values are collected in table 2. (B–D) Determination of the inhibition type of ceritinib at human recombinant CD39 using the MG assay employing 10, 25, 50, 100 and  $150\ \mu\text{M}$  of ATP as a substrate, and 0, 5, 10, 15 and  $20\ \mu\text{M}$  of the inhibitor. (B) Michaelis-Menten plot for the determination of  $V_{\max}$  and  $K_m$  values. (C) Hanes-Woolf plot where the intersection of lines on the X-axis indicates a non-competitive inhibition type. (D)  $V_{\max}$  and  $K_m$  values of CD39 in the presence of the inhibitor ceritinib calculated by GraphPad Prism V.8 from the Michaelis-Menten plot. The  $K_i$  value was calculated to be  $11.0 \pm 0.6\ \mu\text{M}$  by GraphPad Prism V.8 software with non-linear regression of the Michaelis-Menten plot data using the equation  $v_{\max\text{inh}} = v_{\max} / (1 + (I) / K_i)$ .<sup>77</sup> CE, capillary electrophoresis.

the NTPDase family (figure 5).  $IC_{50}$  values were slightly higher at NTPDase3 and NTPDase8 as compared with CD39 (NTPDase1) (figure 5). All results are collected in table 1.

### Effects of ceritinib on the ATPase and AMPase activity of PBMCs

The effect of ceritinib was further investigated on primary human PBMCs. In the donors used for this experiment, the percentage of CD39-expressing PBMCs ranged between 7% and 16% and the percentage of CD73-expressing PBMCs between 11% and 14%. The cells were incubated with the fluorescent CD39 substrate  $1,N^6$ -eATP or the fluorescent CD73 substrate  $1,N^6$ -eAMP in the absence and presence of ceritinib. Fluorescent substrates and products were separated by reversed-phase HPLC coupled to fluorescence detection (excitation: 230 nm, 410 nm emission wavelength), and subsequent quantitative analysis of nucleotides was performed (figure 6A and B). Increasing concentrations of ceritinib resulted in an accumulation of the substrate eATP, while its hydrolysis product eAMP was concomitantly decreased, and its formation was completely blocked at a ceritinib concentration of 50  $\mu$ M and higher (figure 6A).

Ceritinib had only a minor effect on the hydrolysis of eAMP by PBMCs (figure 6B), which is in agreement with our findings on recombinant CD73, which is only weakly inhibited by ceritinib (figure 5A and table 2).

### Effect of ceritinib on the ATPase activity of cancer cell membrane preparations

Hypoxia is a hallmark of the tumor microenvironment, and HIF-1 $\alpha$  induces an overexpression of CD39 and CD73, which contributes to immune escape and a cancer growth-promoting microenvironment.<sup>2</sup> Therefore, we next investigated the effect of ceritinib on ATP hydrolysis by human cancer cell lines, that is, melanoma cells (MaMel65) and TNBC (MDA-MB-231) cells. This TNBC cell line is known to express both CD39 and CD73.<sup>64,65</sup> As expected, ATPase activity of the cancer cell membranes decreased significantly with increasing concentrations of ceritinib (figure 6C). The potency of ceritinib for inhibiting the ATPase activity of both TNBC and melanoma cells was similar to that of the recombinantly expressed CD39, indicating that CD39 is in fact the major enzyme responsible for ATP hydrolysis in these cell lines.

### Effects of ceritinib on the ATPase activity of live cancer cells

Finally, we investigated the inhibitory effects of ceritinib on live cancer cells employing the same human cell lines, TNBC and melanoma cells. Ceritinib displayed a concentration-dependent inhibition of the hydrolysis of eATP added to the cells, which was significant at 10  $\mu$ M (figure 6D). It should be noted, however, that ceritinib, being a potent protein kinase inhibitor, can be cytotoxic at higher concentrations, especially upon extended exposure.

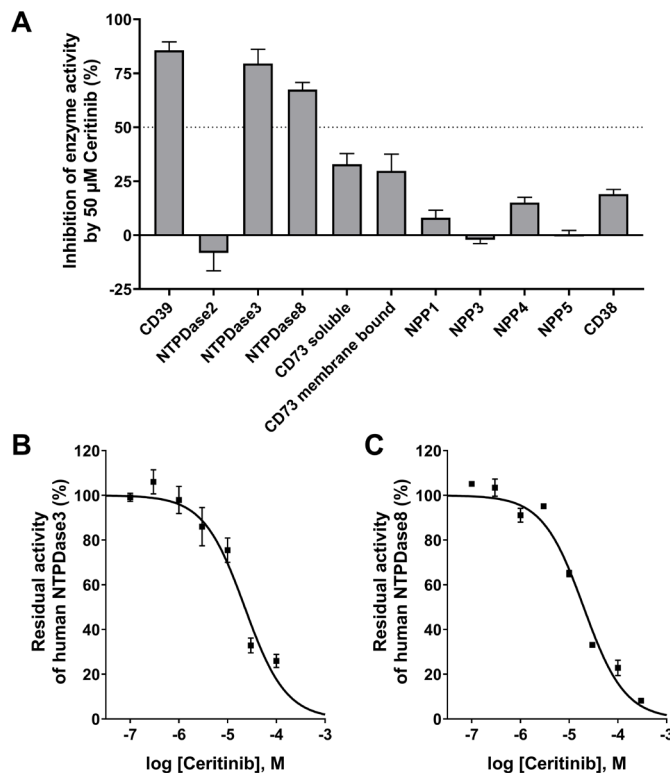


**Figure 5** (A) Inhibition of selected human ectonucleotidases by ceritinib (50  $\mu$ M). (B) and (C) Concentration-dependent inhibition of NTPDase3 (B) and NTPDase8 (C) by ceritinib determined by the malachite green assay applying an ATP substrate concentration of 100  $\mu$ M. For calculated  $IC_{50}$  values see table 1. NPP, nucleotide pyrophosphatase/phosphodiesterase; NTPDase, nucleoside triphosphate diphosphohydrolase.

## DISCUSSION

The screening of protein kinase inhibitors proved to be a successful strategy for the identification of structurally novel CD39 inhibitors; the most potent hit compound was the approved anticancer drug ceritinib. The compound was found to display selectivity for NTPDases within the family of ectonucleotidases, preferably inhibiting NTPDase1 (CD39). Ceritinib displays an allosteric, non-competitive mode of CD39 inhibition. This is in contrast to the inhibition of ALK, where ceritinib was proposed to bind competitively to the ATP binding site of the kinase.<sup>59</sup> The potency of ceritinib as an allosteric CD39 inhibitor is therefore independent of the ATP concentration (see figure 4). This could be a major advantage, since the compound's potency will not be reduced upon the accumulation of extracellular ATP due to the inhibitor's effect on CD39 or due to the release of ATP upon cell death induced by accompanying chemotherapeutics or radiotherapy.<sup>66,67</sup>

At first glance it may appear surprising that ceritinib, which blocks the intracellular ATP binding site of the receptor tyrosine kinase ALK, does not bind to the extracellular orthosteric ATP binding site of CD39, but rather interacts with an allosteric site on CD39, that is presumably located not far from the orthosteric site in the extracellular

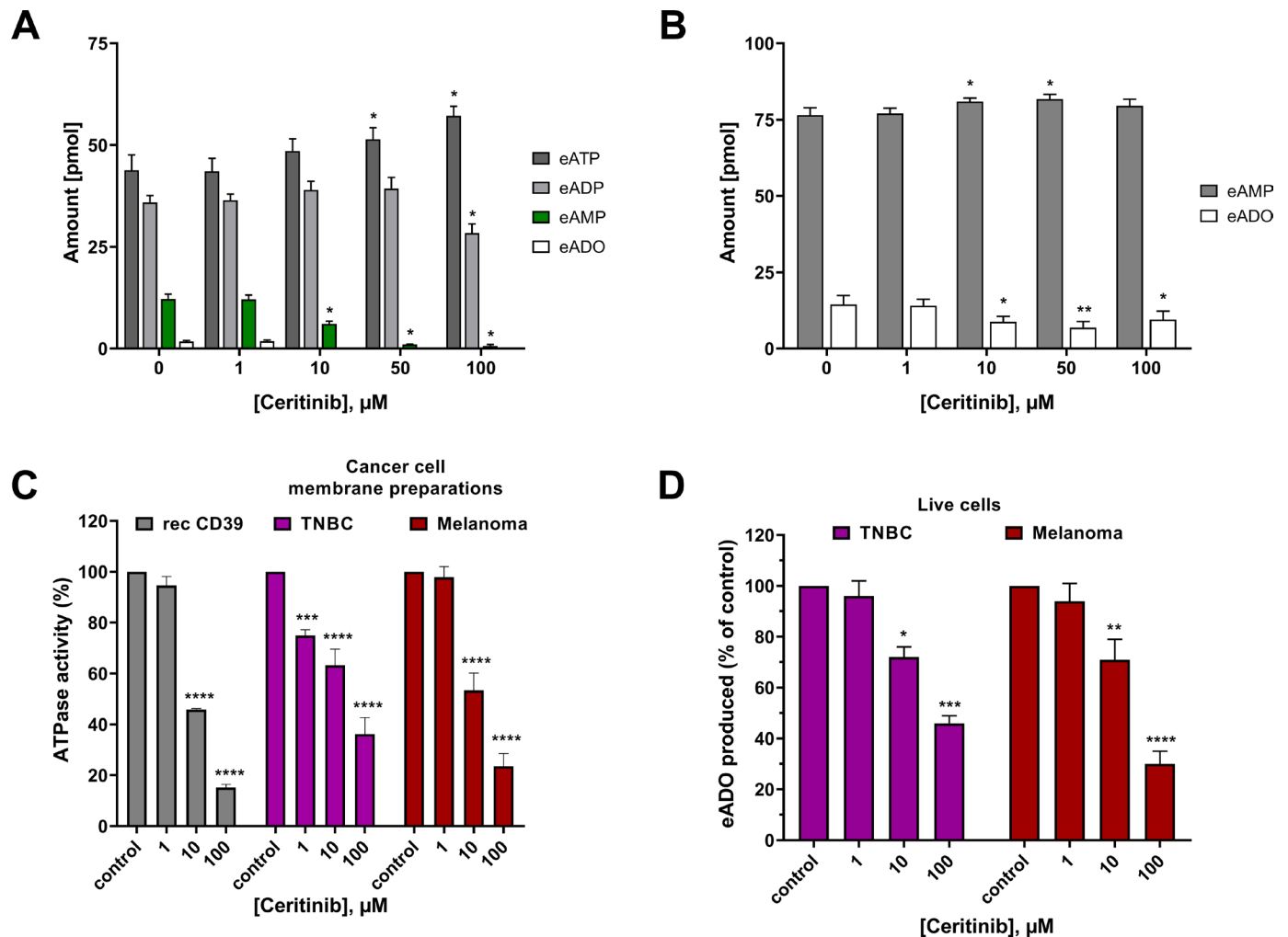


**Figure 6** Hydrolysis of (A) eATP and (B) eAMP by peripheral blood mononuclear cells. Substrate and product concentrations were determined after incubation with or without 1, 10, 50 and 100  $\mu\text{M}$  of ceritinib (singlets,  $n=2-3$ ). (C) ATP hydrolysis by different cell membrane preparations determined by the malachite green assay with 50  $\mu\text{M}$  ATP as substrate in the absence (control) and in the presence of different concentrations of ceritinib (triplicates,  $n=3$ ). (D) Inhibition of the extracellular eATP hydrolysis (20  $\mu\text{M}$ ) by ceritinib (100, 10, and 1  $\mu\text{M}$ ) on live human TNBC (MDA-MB-231) and melanoma (MaMel65) cell lines. The produced eADO was fluorimetrically measured (duplicates,  $n=3$ ) in the presence of the nucleoside transport inhibitor dipyridamole (20  $\mu\text{M}$ ). Rec CD39, recombinant human CD39 expressed in COS-7 cells (gray); TNBC, triple-negative breast cancer cells (violet); melanoma, melanoma cells (red). Data represent means  $\pm$  SEM. The data sets were each analyzed by two-way analysis of variance and Dunnett's multiple comparison test towards the respective control group without ceritinib. Statistical significance: \* $p<0.05$ , \*\* $p<0.01$ , \*\*\* $p<0.001$ , \*\*\*\* $p<0.0001$ . eADO, etheno-adenosine; eADP, etheno ADP; eAMP, etheno AMP; eATP, etheno ATP; TNBC, triple-negative breast cancer.

catalytic domain of the enzyme. Membrane-localized receptors, for example, nucleotide P2Y receptors, have been reported to harbor a so-called meta-binding site which is responsible for the first contact with the physiological ligand, subsequently guiding it to the orthosteric site.<sup>68</sup> Similarly, nucleotide-metabolizing (bacterial) enzymes were described to be allosterically modulated by their substrates, that is, they harbor a second nucleotide binding site.<sup>69</sup> We hypothesize that ceritinib binds to such an allosteric ATP/nucleotide-interacting site in the extracellular domain of CD39 and thereby blocks ATP hydrolysis. The NTPDase1 (CD39) isoenzymes NTPDase3 and NTPDase8, but not NTPDase2, appear to harbor the analogous allosteric binding site since ceritinib inhibited them as well at slightly higher concentrations (about

twofold, see figure 5 and table 2). However, ceritinib was highly selective versus other ectonucleotidase families, including NPPs, CD73, and CD38 (see table 2).

The CD39-inhibitory effects, along with its selectivity versus CD73, were not only observed in recombinant enzyme preparations, but also on native immune as well as cancer cells (figure 6). Ceritinib was proven to inhibit the ability of human cancer cell membrane preparations and PBMCs to dephosphorylate ATP/eATP. Significant effects were observed at TNBC cell membranes already at a concentration of 1  $\mu\text{M}$  leading to reduced ATP degradation (figure 6C). Blood plasma levels of up to 1.4  $\mu\text{M}$  had been determined in patients treated with ceritinib,<sup>61</sup> and local concentrations at the cell membrane, where the enzyme is localized, may be even higher. Ceritinib

**Table 2** Inhibitory potencies of ceritinib on human ectonucleotidases\*

Enzyme	IC <sub>50</sub> ± SEM (μM) (or % inhibition at 50 μM)
Human umbilical cord membrane preparations with high CD39 expression	11.3±0.8
Recombinant human CD39	13.7±0.6 (K <sub>i</sub> =11.0±0.6)†
NTPDase2	>>50 (–8)
NTPDase3	22.7±4.0
NTPDase8	20.3±1.5
Soluble CD73	>50 (33)
Membrane-bound CD73	>50 (30)
NPP1	>>50 (8)
NPP3	>>50 (1)
NPP4	>50 (15)
NPP5	>>50 (1)
CD38	>50 (19)

\*In all cases, three independent experiments were performed. Details on the assays can be found in the Methods Section.

†Determined by non-linear regression of the Michaelis-Menten plot data (see figure 4).

NPP, nucleotide pyrophosphatase/phosphodiesterase; NTPDase, nucleoside triphosphate diphosphohydrolase.

can penetrate cell membranes, the blood-brain barrier, and tumor tissues very well. At a pH of 7.4, it is neutral (uncharged) and therefore quite lipophilic. The piperidine nitrogen (see figure 3B) has weakly basic properties ( $pK_b$  close to 10), which means that it will not be protonated, even in the acidic tumor environment (pH 6.8),<sup>70</sup> remain lipophilic, and keep its excellent ability for tissue permeation. Ceritinib was found to exhibit comparable pharmacokinetics in mice as in humans.<sup>71</sup> In vivo, the drug was found to cross the blood brain barrier and accumulate in brain tumor tissue. In fact, ceritinib appears to accumulate at cell membranes and in tumor tissues, where average concentrations of 36 nmol/g (36 μM) have been observed even in brain tumors under steady-state conditions.<sup>63</sup> The concentration of the drug in some patients reached levels of above 100 μM in tumor tissues, a concentration at which we observed very high or even nearly complete inhibition of CD39 (figures 4A and 6C–D) and of ATP hydrolysis on immune and cancer cells (figure 6). Thus, it is conceivable that ceritinib inhibits CD39 activity – at least in part – in cancer patients treated with the drug. CD39-inhibitory activity might contribute to the potent anticancer effects of ceritinib seen in patients by intercepting hypoxia-induced adenosine signaling leading to a reactivation of T cells. In contrast, two other investigated ALK inhibitors, alectinib and crizotinib, did not inhibit CD39 (see compounds 4 and 13 in table 1 and figure 3).

Ceritinib is, of course, not an ideal CD39 inhibitor due to its very high ALK-inhibitory potency and its inhibition

of some other protein kinases, including the insulin-like growth factor 1 receptor, the insulin receptor, and the serine/threonine protein kinase STK22D (TSSK1).<sup>59</sup> The compound had been found to display growth inhibition and cellular toxicity of tumor cells, which may be dependent on its strong inhibition of ALK and other kinases;<sup>72</sup> ceritinib's cytotoxic mechanism of action may, in fact, be due to its polypharmacology,<sup>73 74</sup> to which CD39 inhibition might additionally contribute.

Nevertheless, our findings are valuable, for example, as a basis for further drug development. In fact, the structure of ceritinib is an excellent starting point for optimization of its CD39-inhibitory potency. Since the structure-activity relationships of ceritinib derivatives and analogs as ALK inhibitors have been extensively studied,<sup>59</sup> it appears to be feasible to reduce or abolish ALK inhibition, and at the same time to increase its CD39-inhibitory potency to obtain potent, selective CD39 inhibitors. Another option would be to design balanced dual ALK/CD39 inhibitors, further increasing CD39-inhibitory activity without compromising ALK inhibition. Such dual ALK/CD39 inhibitors could further improve therapeutic efficacy by combining a targeted anticancer approach (ALK inhibition) with enhanced immunotherapeutic anticancer activity.

Ceritinib is not only the most potent allosteric CD39 inhibitor described to date, moreover, it is the first brain-permeable CD39 inhibitor. Thus, it could be a useful tool compound for further preclinical studies targeting CD39.

Currently, there are only few commercially available CD39 inhibitors that have drug-like physicochemical properties and high metabolic stability. Therefore, ceritinib could be directly considered for further in vitro and in vivo studies targeting CD39 (along with the related NTPDase3 and –8).

Future studies on the structure-activity relationships of ceritinib to optimize its potency at CD39 and to reduce ALK inhibition are warranted.

**Twitter** Christa E Müller @agmueller.unibonn

**Acknowledgements** RW and ET thank Andreas H Guse and Andreas Bauche (Department of Biochemistry and Molecular Cell Biology, University Medical Center Hamburg-Eppendorf (UKE), Hamburg, Germany) for providing the high-performance liquid chromatography system and for assistance with measurements. We thank the Department of Transfusion Medicine (UKE, Hamburg, Germany) for providing blood samples. CM is grateful to Professor Dr Fabio Malavasi, University of Torino, Italy, for providing the complementary DNA of CD38 and for helpful advice.

**Contributors** LS and CM wrote the manuscript with contributions from all coauthors. LS, SM, VL and RI investigated the compounds at ectonucleotidases. RW and ET studied the effect of ceritinib on peripheral blood mononuclear cells. SM performed experiments on live cancer cells. SM and VL expressed and purified nucleotide pyrophosphatase/phosphodiesterases and CD38. JP and JS produced membrane preparations expressing human CD39 and other recombinant NTPDases. HAH generated membrane preparations of human cancer cells. CM designed and supervised the project and is responsible for the overall content as the guarantor.

**Funding** CM, LS and ET were funded by the Deutsche Forschungsgemeinschaft (DFG, German Research Foundation, SFB 1328, Project-ID: 335447717) and by the Federal Ministry of Education and Research (BMBF, project BIGS DrugS). JS received support from the Natural Sciences and Engineering Research Council of Canada (NSERC; RGPIN-2016-05867).

**Competing interests** None declared.

**Patient consent for publication** Consent obtained directly from patient(s).

**Ethics approval** Human PBMCs were isolated from buffy coats obtained from the Department of Transfusion Medicine (Blood Bank) of the University Medical Center Hamburg-Eppendorf (UKE). Blood samples were fully anonymized and donor-related information are not available to the researchers. Human umbilical cords were obtained with consent and under approved institutional review board protocol (Comité d'Éthique de la Recherche du CHU de Québec – Université Laval). Participants gave informed consent to participate in the study before taking part.

**Provenance and peer review** Not commissioned; externally peer reviewed.

**Data availability statement** Data are available upon reasonable request. All data relevant to the study are included in the article or uploaded as supplementary information.

**Open access** This is an open access article distributed in accordance with the Creative Commons Attribution Non Commercial (CC BY-NC 4.0) license, which permits others to distribute, remix, adapt, build upon this work non-commercially, and license their derivative works on different terms, provided the original work is properly cited, appropriate credit is given, any changes made indicated, and the use is non-commercial. See <http://creativecommons.org/licenses/by-nc/4.0/>.

#### ORCID iDs

Laura Schäkel <http://orcid.org/0000-0002-8743-8261>  
 Salahuddin Mirza <http://orcid.org/0000-0002-4944-8282>  
 Riekje Winzer <http://orcid.org/0000-0001-9780-5857>  
 Vittoria Lopez <http://orcid.org/0000-0002-6364-7755>  
 Riham Idris <http://orcid.org/0000-0002-5557-5093>  
 Haneen Al-Hroub <http://orcid.org/0000-0002-2033-0344>  
 Jean Sévigny <http://orcid.org/0000-0003-2922-1600>  
 Christa E Müller <http://orcid.org/0000-0002-0013-6624>

#### REFERENCES

- Allard B, Beavis PA, Darcy PK, *et al.* Immunosuppressive activities of adenosine in cancer. *Curr Opin Pharmacol* 2016;29:7–16.
- Poth JM, Brodsky K, Ehrentauf H, *et al.* Transcriptional control of adenosine signaling by hypoxia-inducible transcription factors during ischemic or inflammatory disease. *J Mol Med* 2013;91:183–93.
- Hatfield SM, Sitkovsky M. A<sub>2A</sub> adenosine receptor antagonists to weaken the hypoxia-HIF-1 $\alpha$  driven immunosuppression and improve immunotherapies of cancer. *Curr Opin Pharmacol* 2016;29:90–6.
- Gao Z-G, Jacobson KA. A<sub>2B</sub> Adenosine Receptor and Cancer. *Int J Mol Sci* 2019;20:5139.
- Borodovsky A, Barbon CM, Wang Y, *et al.* Small molecule AZD4635 inhibitor of A<sub>2A</sub>R signaling rescues immune cell function including CD103<sup>+</sup> dendritic cells enhancing anti-tumor immunity. *J Immunother Cancer* 2020;8:e000417.
- Sitkovsky MV, Hatfield S, Abbott R, *et al.* Hostile, hypoxia-A<sub>2</sub>-adenosinergic tumor biology as the next barrier to overcome for tumor immunologists. *Cancer Immunol Res* 2014;2:598–605.
- Eltzschig HK, Weissmüller T, Mager A, *et al.* Nucleotide metabolism and cell-cell interactions. *Methods Mol Biol* 2006;341:73–87.
- Ohta A, Sitkovsky M. Role of G-protein-coupled adenosine receptors in downregulation of inflammation and protection from tissue damage. *Nature* 2001;414:916–20.
- Ohta A, Gorelik E, Prasad SJ, *et al.* A<sub>2A</sub> adenosine receptor protects tumors from antitumor T cells. *Proc Natl Acad Sci U S A* 2006;103:13132–7.
- Sitkovsky MV. Lessons from the A<sub>2A</sub> adenosine receptor antagonist-enabled tumor regression and survival in patients with treatment-refractory renal cell cancer. *Cancer Discov* 2020;10:16–19.
- Fong L, Hotson A, Powderly JD, *et al.* Adenosine A<sub>2A</sub> receptor blockade as an immunotherapy for treatment-refractory renal cell cancer. *Cancer Discov* 2020;10:40–53.
- Zeng J, Ning Z, Wang Y, *et al.* Implications of CD39 in immune-related diseases. *Int Immunopharmacol* 2020;89:107055.
- Allard B, Allard B, Stagg J. On the mechanism of anti-CD39 immune checkpoint therapy. *J Immunother Cancer* 2020;8:e000186.
- Ghiringhelli F, Bruchard M, Chalmin F, *et al.* Production of adenosine by ectonucleotidases: a key factor in tumor immunoescape. *J Biomed Biotechnol* 2012;2012:1–9.
- Grenz A, Zhang H, Hermes M, *et al.* Contribution of E-NTPDase1 (CD39) to renal protection from ischemia-reperfusion injury. *Faseb J* 2007;21:2863–73.
- Zimmermann H, Zebisch M, Sträter N. Cellular function and molecular structure of ecto-nucleotidases. *Purinergic Signal* 2012;8:437–502.
- Horenstein AL, Chillemi A, Zaccarello G, *et al.* A CD38/CD203A/CD73 ectoenzymatic pathway independent of CD39 drives a novel adenosinergic loop in human T lymphocytes. *Oncoimmunology* 2013;2:e26246.
- Antonoli L, Blandizzi C, Pacher P, *et al.* Immunity, inflammation and cancer: a leading role for adenosine. *Nat Rev Cancer* 2013;13:842–57.
- Zimmermann H. History of ectonucleotidases and their role in purinergic signaling. *Biochem Pharmacol* 2021;187:114322.
- Namasivayam V, Lee S-Y, Müller CE. The promiscuous ectonucleotidase NPP1: molecular insights into substrate binding and hydrolysis. *Biochim Biophys Acta Gen Subj* 2017;1861:603–14.
- Li L, Yin Q, Kuss P, *et al.* Hydrolysis of 2'3'-cGAMP by ENPP1 and design of non-hydrolyzable analogs. *Nat Chem Biol* 2014;10:1043–8.
- Lee S-Y, Müller CE. Nucleotide pyrophosphatase/phosphodiesterase 1 (NPP1) and its inhibitors. *Medchemcomm* 2017;8:823–40.
- Feng L, Sun X, Csizmadia E, *et al.* Vascular CD39/ENTPD1 directly promotes tumor cell growth by scavenging extracellular adenosine triphosphate. *Neoplasia* 2011;13:206–16.
- Turiello R, Capone M, Giannarelli D, *et al.* Serum CD73 is a prognostic factor in patients with metastatic melanoma and is associated with response to anti-PD-1 therapy. *J Immunother Cancer* 2020;8:e001689.
- Allard B, Chrobak P, Allard B, *et al.* Targeting the CD73-adenosine axis in immuno-oncology. *Immunol Lett* 2019;205:31–9.
- Hatfield SM, Sitkovsky MV. Antihypoxic oxygenation agents with respiratory hyperoxia to improve cancer immunotherapy. *J Clin Invest* 2020;130:5629–37.
- Nocentini A, Capasso C, Supuran CT. Small-molecule CD73 inhibitors for the immunotherapy of cancer: a patent and literature review (2017–present). *Expert Opin Ther Pat* 2021;31:867–76.
- Moesta AK, Li X-Y, Smyth MJ. Targeting CD39 in cancer. *Nat Rev Immunol* 2020;20:739–55.
- Kashyap AS, Thelemann T, Klar R, *et al.* Antisense oligonucleotide targeting CD39 improves anti-tumor T cell immunity. *J Immunother Cancer* 2019;7:67.
- Crack BE, Pollard CE, Beukers MW, *et al.* Pharmacological and biochemical analysis of FPL 67156, a novel, selective inhibitor of ecto-ATPase. *Br J Pharmacol* 1995;114:475–81.
- Lévesque SA, Lavoie EG, Lecka J, *et al.* Specificity of the ecto-ATPase inhibitor ARL 67156 on human and mouse ectonucleotidases. *Br J Pharmacol* 2007;152:141–50.
- Schäkel L, Schmiess CC, Idris RM, *et al.* Nucleotide analog ARL67156 as a lead structure for the development of CD39 and dual CD39/CD73 ectonucleotidase inhibitors. *Front Pharmacol* 2020;11:1294.
- Lecka J, Gillerman I, Fausther M, *et al.* 8-BuS-ATP derivatives as specific NTPDase1 inhibitors. *Br J Pharmacol* 2013;169:179–96.
- Baqi Y, Weyler S, Iqbal J, *et al.* Structure-activity relationships of anthraquinone derivatives derived from bromaminic acid as inhibitors of ectonucleoside triphosphate diphosphohydrolases (E-NTPDases). *Purinergic Signal* 2009;5:91–106.
- Müller CE, Iqbal J, Baqi Y, *et al.* Polyoxometalates--a new class of potent ecto-nucleoside triphosphate diphosphohydrolase (NTPDase) inhibitors. *Bioorg Med Chem Lett* 2006;16:5943–7.
- Lee S-Y, Fiene A, Li W, *et al.* Polyoxometalates--potent and selective ecto-nucleotidase inhibitors. *Biochem Pharmacol* 2015;93:171–81.
- Afzal S, Al-Rashida M, Hameed A, *et al.* Functionalized oxindolin hydrazine carbothioamide derivatives as highly potent inhibitors of nucleoside triphosphate diphosphohydrolases. *Front Pharmacol* 2020;11:585876.
- Lecka J, Rana MS, Sévigny J. Inhibition of vascular ectonucleotidase activities by the pro-drugs ticlopidine and clopidogrel favours platelet aggregation. *Br J Pharmacol* 2010;161:1150–60.
- Gardani CFF, Cappellari AR, de Souza JB, *et al.* Hydrolysis of ATP, ADP, and AMP is increased in blood plasma of prostate cancer patients. *Purinergic Signal* 2019;15:95–105.
- Li P, Gao Y, Cao J, *et al.* CD39<sup>+</sup> regulatory T cells attenuate allergic airway inflammation. *Clin Exp Allergy* 2015;45:1126–37.
- Adamiak M, Bujko K, Brzezniakiewicz-Janus K, *et al.* The inhibition of CD39 and CD73 cell surface ectonucleotidases by small molecular inhibitors enhances the mobilization of bone marrow residing stem cells by decreasing the extracellular level of adenosine. *Stem Cell Rev Rep* 2019;15:892–9.
- Côté N, El Hussein D, Pépin A, *et al.* Inhibition of ectonucleotidase with ARL67156 prevents the development of calcific aortic valve disease in warfarin-treated rats. *Eur J Pharmacol* 2012;689:139–46.
- Montalbán Del Barrio I, Penski C, Schlahs L, *et al.* Adenosine-generating ovarian cancer cells attract myeloid cells which differentiate into adenosine-generating tumor associated macrophages - a self-amplifying, CD39- and CD73-dependent

- mechanism for tumor immune escape. *J Immunother Cancer* 2016;4:49.
- 44 Grant SK. Therapeutic protein kinase inhibitors. *Cell Mol Life Sci* 2009;66:1163–77.
- 45 Dancey J, Sausville EA. Issues and progress with protein kinase inhibitors for cancer treatment. *Nat Rev Drug Discov* 2003;2:296–313.
- 46 Noble MEM, Endicott JA, Johnson LN. Protein kinase inhibitors: insights into drug design from structure. *Science* 2004;303:1800–5.
- 47 Sévigny J, Levesque FP, Grondin G, et al. Purification of the blood vessel ATP diphosphohydrolase, identification and localisation by immunological techniques. *Biochim Biophys Acta* 1997;1334:73–88.
- 48 Kukulski F, Lévesque SA, Lavoie EG, et al. Comparative hydrolysis of P2 receptor agonists by NTPDases 1, 2, 3 and 8. *Purinergic Signal* 2005;1:193–204.
- 49 Lopez V, Lee S-Y, Stephan H, et al. Recombinant expression of ecto-nucleotide pyrophosphatase/phosphodiesterase 4 (NPP4) and development of a luminescence-based assay to identify inhibitors. *Anal Biochem* 2020;603:113774.
- 50 Junker A, Renn C, Dobelmann C, et al. Structure-activity relationship of purine and pyrimidine nucleotides as ecto-5'-nucleotidase (CD73) inhibitors. *J Med Chem* 2019;62:3677–95.
- 51 Lowry O, Rosebrough N, Farr AL, et al. Protein measurement with the Folin phenol reagent. *J Biol Chem* 1951;193:265–75.
- 52 Lee S-Y, Luo X, Namasivayam V, et al. Development of a selective and highly sensitive fluorescence assay for nucleoside triphosphate diphosphohydrolase1 (NTPDase1, CD39). *Analyst* 2018;143:5417–30.
- 53 Antonioni L, Blandizzi C, Pacher P, et al. The purinergic system as a pharmacological target for the treatment of immune-mediated inflammatory diseases. *Pharmacol Rev* 2019;71:345–82.
- 54 Cogan EB, Birrell GB, Griffith OH. A robotics-based automated assay for inorganic and organic phosphates. *Anal Biochem* 1999;271:29–35.
- 55 Freundlieb M, Zimmermann H, Müller CE. A new, sensitive ecto-5'-nucleotidase assay for compound screening. *Anal Biochem* 2014;446:53–8.
- 56 Lopez V, Schäkel L, Schuh HJM, et al. Sulfated polysaccharides from macroalgae are potent dual inhibitors of human ATP-hydrolyzing ectonucleotidases NPP1 and CD39. *Mar Drugs* 2021;19:51.
- 57 Lee S-Y, Sarkar S, Bhattarai S, et al. Substrate-dependence of competitive nucleotide pyrophosphatase/phosphodiesterase1 (NPP1) inhibitors. *Front Pharmacol* 2017;8:54.
- 58 Qurishi R, Kaulich M, Müller CE. Fast, efficient capillary electrophoresis method for measuring nucleotide degradation and metabolism. *J Chromatogr A* 2002;952:275–81.
- 59 Marsilje TH, Pei W, Chen B, et al. Synthesis, structure-activity relationships, and in vivo efficacy of the novel potent and selective anaplastic lymphoma kinase (ALK) inhibitor 5-chloro-N2-(2-isopropoxy-5-methyl-4-(piperidin-4-yl)phenyl)-N4-(2-(isopropylsulfonyl)phenyl)pyrimidine-2,4-diamine (LDK378) currently in phase 1 and phase 2 clinical trials. *J Med Chem* 2013;56:5675–90.
- 60 Bossi RT, Saccardo MB, Ardini E, et al. Crystal structures of anaplastic lymphoma kinase in complex with ATP competitive inhibitors. *Biochemistry* 2010;49:6813–25.
- 61 Shaw AT, Kim D-W, Mehra R, et al. Ceritinib in ALK-rearranged non-small-cell lung cancer. *N Engl J Med* 2014;370:1189–97.
- 62 Novartis Pharmaceuticals corporation. *Drug approval package: Zykadia (ceritinib) capsules*, 2014. [https://www.accessdata.fda.gov/drugsatfda\\_docs/nda/2014/205755Orig1s000TOC.cfm](https://www.accessdata.fda.gov/drugsatfda_docs/nda/2014/205755Orig1s000TOC.cfm)
- 63 Mehta S, Fiorelli R, Bao X, et al. A phase 0 trial of ceritinib in patients with brain metastases and recurrent glioblastoma. *Clin Cancer Res* 2022;28:289–97.
- 64 Bastid J, Regairaz A, Bonnefoy N, et al. Inhibition of CD39 enzymatic function at the surface of tumor cells alleviates their immunosuppressive activity. *Cancer Immunol Res* 2015;3:254–65.
- 65 Petruk N, Tuominen S, Åkerfelt M, et al. CD73 facilitates EMT progression and promotes lung metastases in triple-negative breast cancer. *Sci Rep* 2021;11:6035.
- 66 de Leve S, Wirsdörfer F, Jendrossek V. Targeting the immunomodulatory CD73/adenosine system to improve the therapeutic gain of radiotherapy. *Front Immunol* 2019;10:698.
- 67 Schneider G, Glaser T, Lameu C, et al. Extracellular nucleotides as novel, underappreciated pro-metastatic factors that stimulate purinergic signaling in human lung cancer cells. *Mol Cancer* 2015;14:201.
- 68 Moro S, Hoffmann C, Jacobson KA. Role of the extracellular loops of G protein-coupled receptors in ligand recognition: a molecular modeling study of the human P2Y1 receptor. *Biochemistry* 1999;38:3498–507.
- 69 Velloso LM, Bhaskaran SS, Schuch R, et al. A structural basis for the allosteric regulation of non-hydrolysing UDP-GlcNAc 2-epimerases. *EMBO Rep* 2008;9:199–205.
- 70 Zhang X, Lin Y, Gillies RJ. Tumor pH and its measurement. *J Nucl Med* 2010;51:1167–70.
- 71 Kang CH, Kim E-Y, Kim HR, et al. Minor modifications to ceritinib enhance anti-tumor activity in EML4-ALK positive cancer. *Cancer Lett* 2016;374:272–8.
- 72 Kawauchi D, Takahashi M, Satomi K, et al. The ALK inhibitors, alectinib and ceritinib, induce ALK-independent and STAT3-dependent glioblastoma cell death. *Cancer Sci* 2021;112:2442–53.
- 73 Kuenzi BM, Remsing Rix LL, Stewart PA, et al. Polypharmacology-based ceritinib repurposing using integrated functional proteomics. *Nat Chem Biol* 2017;13:1222–31.
- 74 Petrazzuolo A, Perez-Lanzon M, Martins I, et al. Pharmacological inhibitors of anaplastic lymphoma kinase (ALK) induce immunogenic cell death through on-target effects. *Cell Death Dis* 2021;12:713.
- 75 Khozin S, Blumenthal GM, Zhang L, et al. FDA approval: ceritinib for the treatment of metastatic anaplastic lymphoma kinase-positive non-small cell lung cancer. *Clin Cancer Res* 2015;21:2436–9.
- 76 Huang W-S, Metcalf CA, Sundaramoorthi R, et al. Discovery of 3-[2-(imidazo[1,2-b]pyridazin-3-yl)ethynyl]-4-methyl-N-{4-[(4-methylpiperazin-1-yl)methyl]-3-(trifluoromethyl)phenyl}benzamide (AP24534), a potent, orally active pan-inhibitor of breakpoint cluster region-abelson (BCR-ABL) kinase including the T315l gatekeeper mutant. *J Med Chem* 2010;53:4701–19.
- 77 Copeland RA. *Enzymes: a practical introduction to structure, mechanism, and data analysis*. 2nd edn. Wiley-VCH, Inc, 2000.